



Studies on Mg-Al oxide hydrotalcite supported Pd catalysts for vapor phase hydrogenation of nitrobenzene

P. Sangeetha^a, P. Seetharamulu^b, K. Shanthi^a, S. Narayanan^b, K.S. Rama Rao^{b,*}

^a Department of Chemistry, Anna University, Chennai 600025, India

^b Inorganic and Physical Chemistry Division, Indian Institute of Chemical Technology, Hyderabad 500007, India

Received 22 January 2007; received in revised form 5 March 2007; accepted 6 March 2007

Abstract

Pd supported on Mg-Al hydrotalcite with different Pd loadings (0.5, 1, 2 and 5 wt.% of Pd) prepared by impregnation method were characterized by XRD, BET Surface area, CO chemisorption and TPR. The catalyst activity was studied for vapor phase hydrogenation of nitrobenzene at atmospheric pressure in the temperature range of 498–598 K. The metallic dispersion, was obtained by CO chemisorption studies. Pd particle size before and after the reaction was calculated from XRD data. From the TPR studies, it was observed that the negative signal due to the decomposition of PdH_x in the low temperature region was absent due to the smaller particle size of the Pd. XRD result also indicate the presence of smaller Pd particle size in low Pd loadings which increases with Pd loading. It was observed that very low concentration of Pd supported on hydrotalcite (0.5 wt.% Pd/HT) is sufficient to get high activity towards the hydrogenation of nitrobenzene to aniline (conversion = 97% and selectivity = 98%) at 498 K. The higher activity of this catalyst was attributed to higher dispersion and lower particle size of Pd as observed from CO chemisorption and XRD results. The particle size of Pd before and after reaction is more or less same indicating that the deactivation is not due to Pd agglomeration but due to the poisoning effect of water generated during the course of the reaction. The reconstruction of hydrotalcite structure in the spent catalysts as evidenced by XRD is indication that water is formed during the reaction.

© 2007 Published by Elsevier B.V.

Keywords: Hydrotalcite; Palladium; Hydrogenation; Nitrobenzene; Aniline

1. Introduction

Supported metal catalysts are widely used for hydrogenation of many organic compounds [1]. Among supported noble metal catalysts, palladium is one of the most frequently used metals for hydrogenation reactions at laboratory as well as industrial scale. Hydrotalcite, a class of basic mixed hydroxides, has been tried as support for dispersing noble metals [2–7]. HT like compounds have been proved as good support precursors for hydrogenation catalysts and are gaining importance in base catalyzed reactions and also as supports for dispersing metals [8]. Clays, especially synthetic anionic clays of hydrotalcite type, have found application as catalyst support for precious metals. It has been found that the basic nature as well as the exchangeable property of cation in the brucite layer of hydrotalcite support is useful for metal dispersion, which is responsible for hydrogenation reaction.

Aniline is an important raw material used for the production of methylene diphenyl diisocyanate (MDI). It is also used as additive for rubber process, intermediate dyes and pigments, pesticides and herbicides. About 85% of global aniline is produced by catalytic hydrogenation of nitrobenzene. Carbon nanotube supported platinum catalyst has been used for the hydrogenation of nitrobenzene [9]. Platinum nanoparticle core-polyaryl ether trisacetic acid ammonium chloride dendimer shell nanocomposites were employed for hydrogenation of nitrobenzene to aniline with molecular hydrogen under mild conditions [10]. Active carbons were used as supports for palladium in the liquid phase hydrogenation of nitrobenzene to aniline [11]. Hydrogenation of nitrobenzene was studied over Pt/C catalysts in supercritical carbon dioxide and ethanol [12]. Polymer anchored metal complex catalyst has been used for the hydrogenation of nitrobenzene [13]. Liquid phase hydrogenation of nitrobenzene was studied over Pd-B/SiO₂ amorphous catalyst [14].

The aim of the present work is to study the catalytic activity for vapour phase hydrogenation of nitrobenzene using Pd supported hydrotalcite catalyst at atmospheric pressure with

* Corresponding author. Tel.: +91 40 27160123; fax: +91 40 27160921.
E-mail address: ksramarao@iict.res.in (K.S. Rama Rao).

different loadings (0.5, 1, 2 and 5 wt.% of Pd). The catalytic activity results were discussed in terms of characteristics such as Pd particle size and metal dispersion.

2. Experimental

2.1. Preparation of catalysts

All the chemicals were obtained from M/S. Merck India.

2.1.1. Preparation of support

Mg–Al hydrotalcite (HT) was prepared according to the method reported by Reichle et al. [15]. Briefly, solution A was prepared by dissolving 256 g of $\text{Mg}(\text{NO}_3)_2 \cdot 6\text{H}_2\text{O}$ (1 mol) and 185.7 g of $\text{Al}(\text{NO}_3)_3 \cdot 9\text{H}_2\text{O}$ (0.5 mol) in 700 cm³ distilled water, maintaining a Mg/Al molar ratio of 2. Solution B was prepared by dissolving 280 g of 50% NaOH (140 g in 140 cm³ distilled water) and 100 g of Na_2CO_3 in 1000 cm³ distilled water. HT was prepared by adding solution A to solution B in 3–4 h with constant stirring while maintaining the pH between 11 and 13. The resulting gel was transferred to an autoclave and allowed to crystallise at 333 K for 18 h. The sample was filtered and washed several times with hot distilled water until pH of the filtrate is neutral and also to remove any free sodium ions that may be present. The sample was dried in an oven for 12 h at 373 K and then calcined at 723 K in air for 18 h to get the hydrotalcite (HT).

2.1.2. Preparation of Pd/HT catalysts

A 0.5 wt.% Pd on HT support was prepared by an incipient wetness impregnation method, using an aqueous solution of palladium chloride acidified with HCl (to effect the complete dissolution of the salt) to deposit Pd on HT. The resulting slurry was stirred well for removing excess water and subsequently dried in an oven at 373 K for 12 h. The solid residue was then crushed and calcined in air at 723 K for 5 h. Similarly 1, 2 and 5 wt.% Pd on hydrotalcite support were prepared.

2.2. Characterisation

BET surface area of the catalysts were obtained on an Autosorb Automated Gas Sorption System (M/s. Quantachrome, USA) with physical adsorption of N_2 at liquid nitrogen temperature. X-ray powder diffraction (XRD) patterns of all catalysts were recorded on a Rigaku Miniflex (M/s. Rigaku Corporation, Japan) X-ray diffractometer using Ni filtered $\text{Cu K}\alpha$ radiation ($\lambda = 1.5406 \text{ \AA}$) with a scan speed of 2° min^{-1} and a scan range of $2\text{--}80^\circ$ at 30 kV and 15 mA. Pd particle size was calculated from the raw XRD patterns by using Debye–Sherrer equation. Temperature programmed reduction (TPR) profiles of the catalysts were generated on a home made on-line quartz micro reactor interfaced to a thermal conductivity detector (TCD) equipped with a gas chromatograph (Varian CP 3800 USA) and the profiles were recorded using GC software. H_2/Ar (10 vol.% of H_2 and balance Ar) mixture was used as the reducing gas while the catalyst (100 mg) was heated at a linear heating ramp of 10 K min^{-1} from 303 to 850 K.

CO chemisorption was carried out at 303 K on a homemade pulse reactor to evaluate the dispersion and metal particle size. In a typical experiment, about 100 mg of the catalyst sample was placed in a micro-reactor of 8 mm i.d., and 250 mm long quartz reactor and the catalyst sample was first reduced under a hydrogen flow at 673 K for 2 h, pre-treatment at 673 K for 1 h under He flow and finally was cooled in He flow up to 303 K. The outlet of the reactor was connected to a micro-thermal conductivity detector (TCD) equipped in GC-17A (M/s. Shimadzu Instruments, Japan) through an automatic six-port valve (M/s. Valco Instruments U.S.A.). After cooling, pulses of 10% CO balance He were injected at room temperature through a 1 ml loop connected to the six-port valve until no further change in the intensity of the outlet CO (from GC-software). Assuming CO:Pd stoichiometry of 1:1, dispersion of Pd were calculated.

2.3. Nitrobenzene hydrogenation

Vapour phase hydrogenation of nitrobenzene reaction was performed in a fixed-bed tubular reactor (10 mm i.d., 300 mm long glass reactor) using 0.5 g catalyst at atmospheric pressure and at different temperatures ranging from 498 to 573 K. The catalyst sample was packed at the center of reactor between two plugs of quartz wool and quartz beads were placed above the catalyst bed to act as a preheating zone. The catalyst has been reduced in a flow of H_2 at 673 K for 3 h under H_2 flow. Nitrobenzene (1 ml h^{-1}) is injected continuously with the help of a syringe pump (Secura FT, M/S. B. Braun Germany) and H_2 (>99.9% pure) flow (1 l h^{-1}) is maintained. The product mixture was collected every hour in an ice-cold trap and analyzed by a GC (GC-17A, M/S. Shimadzu instruments, Japan) using a Zebron ZB-WAX capillary column of 0.53 mm diameter and 30 m long.

3. Results and discussion

3.1. Characterisation

BET surface area, CO uptake, Pd dispersion and Pd particle size (reduced and spent catalysts) of supported palladium catalysts with different loadings are given in Table 1. Calcined hydrotalcite support has a surface area of about $214 \text{ m}^2 \text{ g}^{-1}$. The loss of interstitial water and the loss of carbon dioxide and water due to decarbonation and dehydroxylation leads to amorphous oxide with high surface area in calcined hydrotalcite [15]. As the loading of Pd increases from 0.5 to 5 wt.% surface area is found to decrease. Surface area of 0.5 wt.% Pd/HT is found to be $198 \text{ m}^2 \text{ g}^{-1}$. The surface area decreases due to the increase in metal loading onto the support due to the pore blocking by bigger Pd particles.

Fig. 1 shows XRD patterns of reduced Pd/HT catalysts with different loadings of Pd. MgO periclase phase (ICDD No. 87-0653, $d = 2.09, 1.49, 1.20$) and metallic Pd phases (ICDD No. 87-0638, $d = 2.25, 1.95, 1.38$) are observed from XRD patterns of the reduced catalysts. From Fig. 1, it is clearly observed that 0.5 wt.% Pd/HT catalyst shows low intense signal corresponding to metallic Pd phase. This indicates that the Pd metal particle size is small because of high dispersion. As the loading increases the

Table 1
Surface area, dispersion, and particle size of supported palladium catalysts

Catalyst	Surface area (m ² g ⁻¹)	CO uptake (μmol g ⁻¹)	Dispersion (%) ^a	Particle size (Å) ^b	
				Reduced	Spent
0.5% Pd/HT	198	40	86	19.7	20.6
1% Pd/HT	183	68	72	25.42	27.8
2% Pd/HT	174	93	49	32	36.19
5% Pd/HT	152	141	30	47.14	64.03

^a Calculated as [CO uptake (μmol g⁻¹) × 100]/[total Pd (μmol g⁻¹)].

^b Calculated from XRD using Debye–Scherrer equation: $d = K\lambda/\beta \cos \theta$.

intensity of the metallic palladium phase increases. XRD patterns of spent catalysts are shown in Fig. 2 which clearly indicate that the hydrotalcite phase [ICDD No. 22-700, $d = 7.84, 3.90, 2.57$] is reconstructed in all the catalysts after the reaction [16]. The reason may be due to absorption of water vapour, which is released in the reaction as a byproduct, and hence the catalysts regain hydrotalcite structure back by memory effect [17]. A keen observation of the XRD patterns reveal that the intensities of hydrotalcite reflections is decreasing upon increase in metal loading. Pd particle size in reduced and spent catalysts are calculated from the raw XRD data with silica grid reference sample using Debye–Scherrer equation, $d = K\lambda/\beta \cos \theta$ where K is assumed to be 1 and λ is the wavelength of Cu K α radiation is 1.5408 Å. β is the difference between the full width

at half maximum (FWHM) values of maximum intense signal in the catalyst sample and that of silica grid at same 2θ values.

TPR profiles of palladium hydrotalcite catalysts (0.5, 1, 2 and 5 wt.%) are shown in Fig. 3. A two-stage reduction is observed in all the catalysts. The first stage reduction gives rise to a strong positive hydrogen consumption peak at $T_{\max} \sim 425$ K. This represents PdO reduction and/or hydrogen chemisorption on the metallic palladium that is formed and/or hydrogen adsorption that is known to occur directly on the support as well as spillover species [18,19]. The second stage reduction at $T_{\max} \sim 760$ K indicates further consumption of hydrogen on all the catalysts, which may be attributed to the spill over of the hydrogen activated on metallic palladium on to the support [20]. No negative peak corresponding to β -PdH_x decomposition in the low temperature region is observed over Pd/HT catalysts. The reason may be due to high dispersion of palladium over the support [21]. The increase in the H₂ signal intensity in the lower tem-

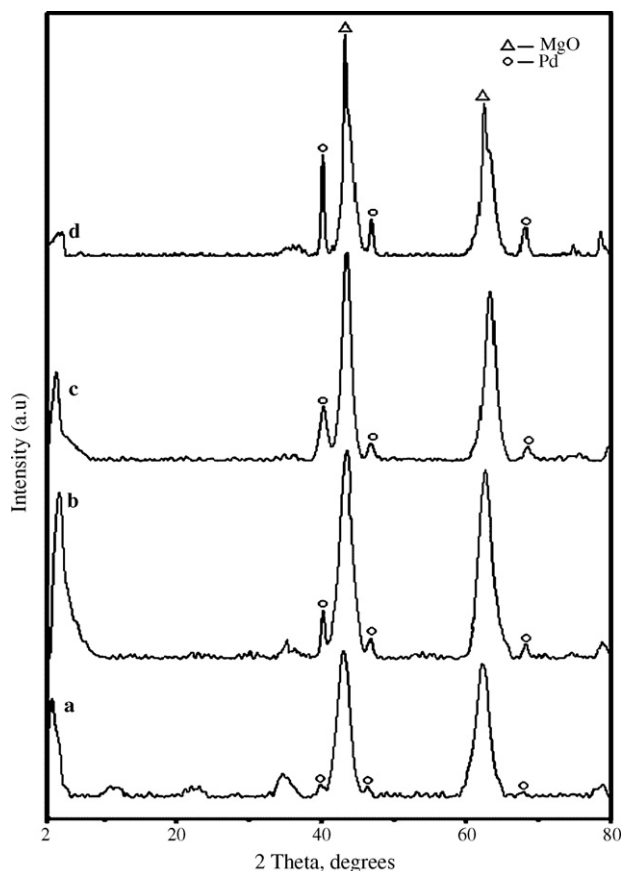


Fig. 1. XRD patterns of reduced hydrotalcite supported Pd catalysts (a) 0.5 wt.%, (b) 1 wt.%, (c) 2 wt.% and (d) 5 wt.%.

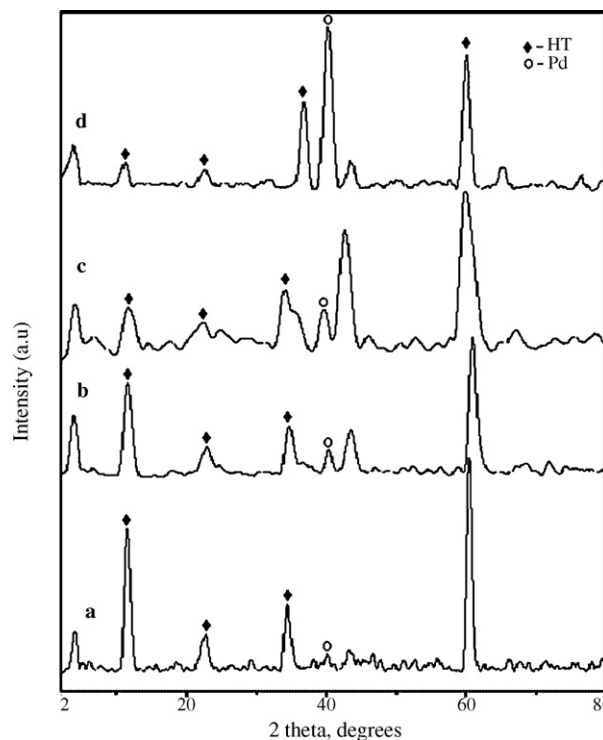


Fig. 2. XRD patterns of spent hydrotalcite supported Pd catalysts (a) 0.5 wt.%, (b) 1 wt.%, (c) 2 wt.% and (d) 5 wt.%.

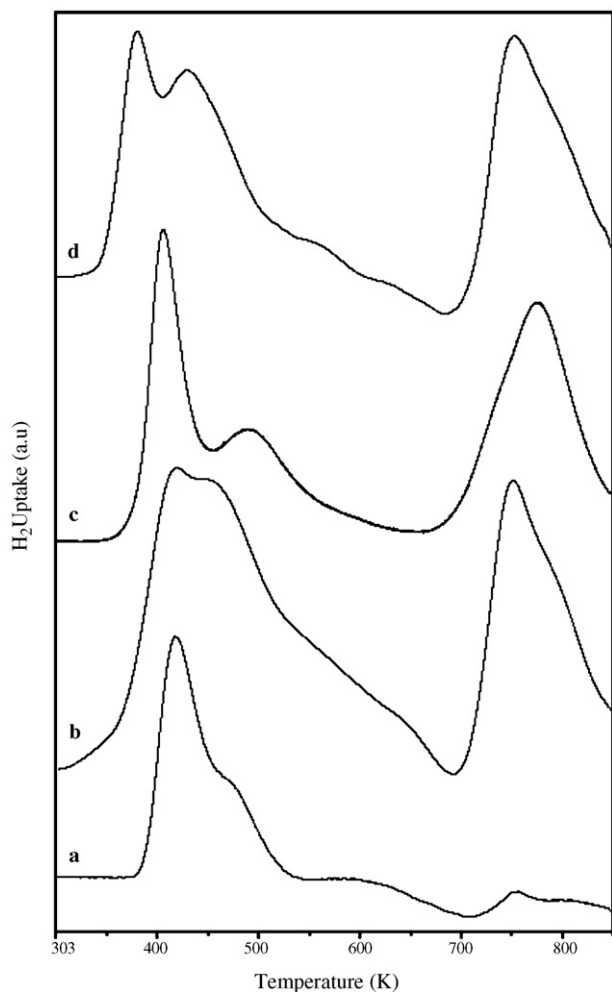


Fig. 3. TPR profiles of calcined Pd/HT catalysts (a) 0.5 wt.%, (b) 1 wt.%, (c) 2 wt.% and (d) 5 wt.%.

perature and higher temperature regions is due to the higher Pd loadings.

The physical characteristics of palladium catalysts with different loadings (0.5, 1, 2 and 5 wt.%) of Pd on hydrotalcite support are given in Table 1. The adsorption of carbon monoxide on palladium has attracted much attention because CO is an interesting probe molecule to characterize adsorption sites [22]. Dispersion of a supported palladium catalysts are calculated by CO chemisorption studies. Increase in Pd loading on HT support promotes sintering which in turn leads to the decreased dispersion. Palladium disperses well on hydrotalcite support than other conventional supports such as MgO and γ -alumina [23]. Table 1 shows the Pd dispersion from CO chemisorption and particle size before and after reaction from XRD. A 0.5 wt.% Pd/HT shows high dispersion among all the catalysts. As the loading increases from 0.5 to 5 wt.%, the dispersion decreases and correspondingly the metal particle size increases. This may be probably, due to decrease in surface area with increase in Pd loading, which is also observed in XRD patterns. It is interesting to observe that there is not much significant variation in the Pd particle size before and after the reaction except in the catalyst with high Pd loading.

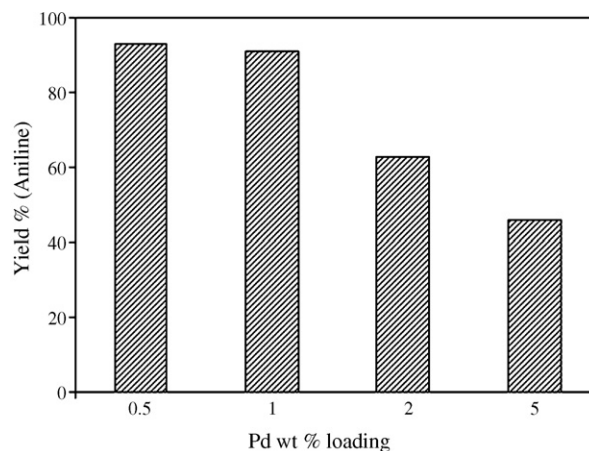


Fig. 4. Effect of Pd loading in the hydrogenation of nitrobenzene over Pd/HT catalysts; T : 498 K, catalyst: 0.5 g, GHSV: 1500 h^{-1} , H_2 flow: 1 h^{-1} .

3.2. Catalytic activity

3.2.1. Effect of loadings on conversion and selectivity

Fig. 4 shows the effect of loading on the yield of aniline. As the loading increases from 0.5 to 5 wt.% the yield decreases. It is observed that 0.5 wt.% Pd/HT shows higher yield (93%). This is due to higher dispersion of Pd (86%) and smaller particle size of Pd. A 1 wt.% Pd/HT shows a yield of (91%). But in the case of 2 wt.% Pd/HT and 5 wt.% Pd/HT the yield of aniline is 63 and 46%, respectively. The decrease in the yield is due to lower dispersion and larger particle size of Pd, which is clearly observed from CO chemisorption and XRD studies (Table 1). It was reported that the high dispersion and smaller particle size of Pd in Pd/carbon catalysts showed higher reaction rates of nitrobenzene in presence of methanol or isopropanol as solvents [24]. High dispersed Pt catalysts are reported to be helpful to obtain nitrobenzene hydrogenation activity under mild reaction conditions [9]. It is reported that the catalytic activity of nitrobenzene hydrogenation correlates well with the Pd metal area [14]. Smaller Pd particles possess greater Pd areas.

3.2.2. Effect of temperature

The vapour phase hydrogenation of nitrobenzene yields aniline and water as per the reaction in Scheme 1. The reaction was studied over different loadings of palladium (0.5, 1, 2 and 5 wt.%) on hydrotalcite support in the temperature range of 498–573 K. Fig. 5 shows the influence of reaction temperature on the activity and selectivity for hydrotalcite supported palladium catalyst. A 0.5 wt.% Pd/HT shows higher conversion of 97% at lower temperature of 498 K. Among all the (0.5,



Scheme 1. Reaction scheme of nitrobenzene hydrogenation.

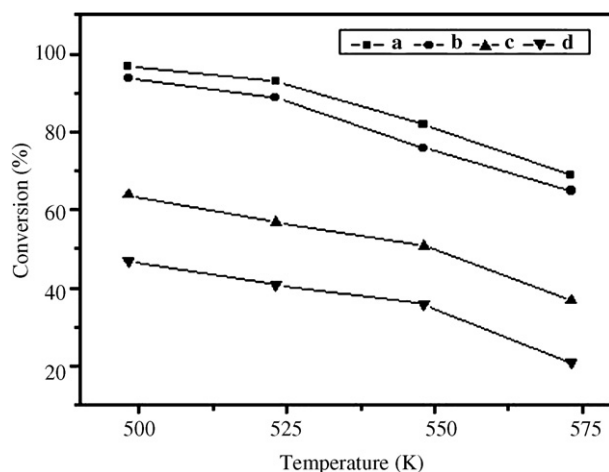


Fig. 5. Effect of temperature on nitrobenzene conversion over Pd/HT catalysts; catalyst: 0.5 g, GHSV: 1500 h⁻¹, H₂ flow: 11 h⁻¹.

1, 2 and 5 wt.%) Pd/HT catalysts, the conversion is found to be higher for 0.5 wt.% Pd/HT. As the temperature increases conversion is found to decrease in all the catalysts. Nitrobenzene hydrogenation is exothermic reaction (heat of reaction, $\Delta H = -130$ kcal/mol). Hence, the reaction is favorable at lower reaction temperatures. The other reason may be agglomeration of Pd sites to give bigger Pd particles. However, the particle size of Pd in the spent catalysts is more or less same as that in the fresh catalysts except in the 5 wt.% Pd/HT catalyst. Hence agglomeration of Pd during the course of the reaction is ruled out. Thus, the optimum temperature is found to be 498 K for the 0.5 wt.% Pd/HT catalyst, which shows maximum conversion. This may be attributed to very high dispersion of Pd (86%) on hydrotalcite support in this catalyst. Thus, the calcined hydrotalcite supported Pd catalyst (0.5 wt.%) has got higher BET surface area, higher Pd dispersion and smaller Pd particle size and hence superior activity is observed in this catalyst. In the case of 1 wt.% Pd/HT the conversion is found to be 94% and there is a decrease in conversion with increase in temperature. In the case of 2 wt.% and 5 wt.% Pd/HT the conversion is found to be low even at lower temperatures, which may be due to bigger particle size of Pd.

3.2.3. Effect of time on stream

Fig. 6 shows variation in conversion against time on stream over Pd/HT catalysts. The conversion is found to be more or less same up to 3 h, indicating a stable activity of the catalyst. After 3 h, there is a decrease in conversion with time. From XRD of spent catalysts, it is observed that there is a reconstruction of hydrotalcite phase after the reaction, which shows that water is helpful for the formation of HT phase. However, the formation of water may be a poison for the catalyst because of which the activity loss might have occurred. Since the Pd particle size in reduced and spent catalysts is more or less same, the activity loss either during the time on stream or against temperature due to agglomeration of Pd is ruled out. Hence it is better to speculate that generation of water causes deactivation.

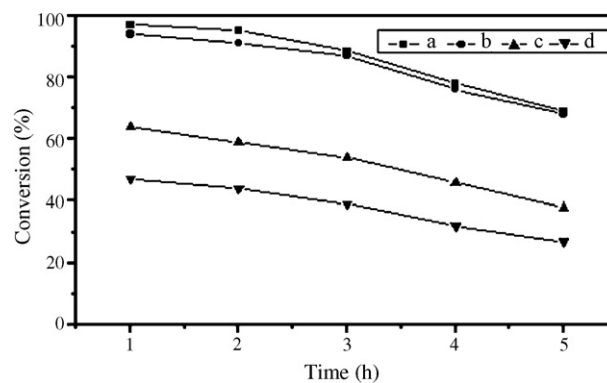


Fig. 6. Effect of time on stream over Pd/HT catalysts. T: 498 K, catalyst: 0.5 g, GHSV: 1500 h⁻¹, H₂ flow: 11 h⁻¹.

3.2.4. Turn over frequency (TOF)

The turn over frequency (TOF) of nitrobenzene conversion on each catalyst is defined as the number of molecules of nitrobenzene converted per one surface Pd atom per second. It is calculated as,

$$\text{TOF} = \frac{\text{number of moles of nitrobenzene passed per second} \times \text{fractional conversion}}{\text{number of surface Pd sites}}$$

Number of surface Pd sites is assumed to be equal to the number of CO moles adsorbed per gram of catalyst. Since the TOF against Pd loading at different temperatures follows an exponential decay curve a plot between 1/TOF versus Pd loading is drawn (Fig. 7). This figure indicates that 1/TOF increases with Pd loading. However, at lower Pd loadings, 1/TOF is more or less same for all the catalysts and at all the temperatures. Extrapolation of this curve up to zero Pd loading gives an intercept on Y-axis at a value of ~ 2 at all temperatures. Thus, the true turn over frequency (TTOF) at a near zero Pd loading which is assumed to be the true activity on one Pd atom present on HT support is 0.5. In other words, a catalyst with one Pd atom on HT support converts 5 nitrobenzene molecules in 1 s, at all the temperatures studied.

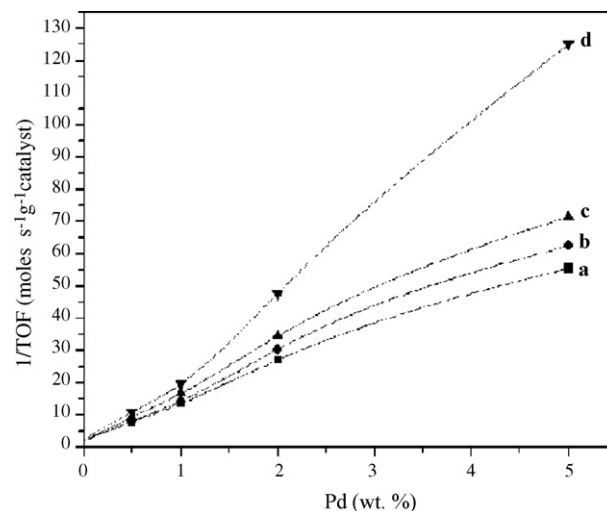


Fig. 7. A plot between 1/TOF vs. Pd loading (a) 498 K, (b) 523 K, (c) 548 K and (d) 573 K. Catalyst: 0.5 g, GHSV: 1500 h⁻¹, H₂ flow: 11 h⁻¹.

However, as the Pd content increases the TOF value decreases because of the agglomeration. The bigger particle size of Pd in 5 wt.% Pd/HT catalyst is the reason for its lower TOF value. At lower Pd loadings there is not much variation in the TOF values against rise in reaction temperature. This is because of smaller Pd particle size with high dispersion. However, the contribution of Pd surface area in the total surface area is $\leq 1\%$ in the catalysts with lower Pd contents (0.5–1 wt.% Pd/HT catalysts). In the other words, even though the smaller Pd particles at lower loadings reside predominantly on the surface rather than in bulk (dispersion is $>70\%$ below 1 wt.% Pd/HT), their contribution in the total area is small and there is enough area to accommodate further Pd loading. At higher Pd loading of 5 wt.%, the Pd surface area contribution to the overall area is $<4\%$ with bigger Pd particles (47 Å). Thus, it seems the available surface on HT is not uniform. Only on certain portion of the surface, Pd particles are getting deposited without forming a complete monolayer. It is reported that during the impregnation of HT with acidified PdCl₂ solution, PdCl₄²⁻ replaces the CO₃⁻ interlayer anions at the edges yielding a good dispersion of Pd on reduction [6]. Thus, it appears the dispersion of Pd depends on the amount of interlayer anions. Further studies are required to find out the ways to increase the Pd dispersion on HT support.

4. Conclusion

The effect of dispersion and particle size of palladium supported on hydrotalcite in the hydrogenation activity of these catalysts in the conversion of nitrobenzene to aniline is significant. It is observed that catalyst with 0.5 wt.% Pd loading on hydrotalcite has been found to be more selective and active over the other catalysts studied. The reason for the higher activity shown by 0.5 wt.% Pd/HT (conversion = 97% and selectivity = 98%) has been attributed to the higher dispersion and lower particle size of Pd as observed from the CO chemisorption and XRD studies. Thus, hydrotalcite supported palladium catalyst has been found to be an effective catalyst in the synthesis of aniline from the hydrogenation of nitrobenzene. However, the deactivation either during the rise in temperature or during the time on stream is not due to agglomeration of Pd which is evidenced from more or less same Pd particle size from XRD

of catalysts before and after reaction. The absence of negative signal in the lower temperature region due to the decomposition of PdH_x species in the TPR pattern clearly indicates the presence smaller Pd particles. The deactivation may be due to water generated during the course of reaction.

Acknowledgements

The authors thank Dr. J.S. Yadav, Director, Indian Institute of Chemical Technology, Hyderabad, India for permitting to publish the work. The authors thank Dr. M. Lakshmikantham, Head, I&PC division for her support in this work. One of the author P.S. thanks DRDO, New Delhi for a research fellowship.

References

- [1] F. Solymosi, Catal. Rev. 1 (1968) 252.
- [2] R.J. Davis, E.G. Derouane, J. Catal. 132 (1991) 269.
- [3] R.J. Davis, E.G. Derouane, Nature 349 (1991) 313.
- [4] S. Narayanan, K. Krishna, Appl. Catal. A: Gen. 198 (2000) 13.
- [5] S. Narayanan, K. Krishna, Appl. Catal. A: Gen. 147 (1996) L253.
- [6] S. Narayanan, K. Krishna, Chem. Commun. (1997) 1991.
- [7] S. Narayanan, K. Krishna, Catal. Today 49 (1999) 57.
- [8] F. Cavani, F. Trifiro, A. Vaccari, Catal. Today 11 (1991) 173.
- [9] C.H. Li, Z.X. Yu, K.F. Yao, S.F. Ji, J. Liang, J. Mol. Catal. A: Chem. 226 (2005) 101.
- [10] P. Yang, W. Zhang, Y. Du, X. Wang, J. Mol. Catal. A: Chem. 260 (2006) 4.
- [11] N. Bouchenafa-Saib, P. Grange, P. Verhasselt, F. Addoun, V. Dubois, Appl. Catal. A: Gen. 286 (2005) 167.
- [12] F. Zhao, Y. Ikushima, M. Arai, J. Catal. 224 (2004) 479.
- [13] D.R. Patel, R.N. Ram, J. Mol. Catal. A: Chem. 130 (1998) 57.
- [14] X. Yu, M. Wang, H. Li, Appl. Catal. A: Gen. 202 (2000) 17.
- [15] W.T. Reichle, S.Y. Kang, D.S. Everhardt, J. Catal. 101 (1986) 352.
- [16] S. Miyata, Clays Clay Miner. 23 (1975) 369.
- [17] D. Tichit, B. Coq, Cattech. 6 (2003) 206.
- [18] D. Ercole A. E. Giannelo, C. Disani, L. Ojamae, J. Phys. Chem. B 103 (1999) 3872.
- [19] P. Claus, H. Berndt, C. Mohr, J. Radnik, E.T. Shin, M.A. Keane, J. Catal. 192 (2000) 88.
- [20] T. Itoh, M. Kusamoto, M. Yoshida, T. Tokuda, J. Phys. Chem. 87 (1983) 4411.
- [21] A.H. Padmasri, A. Venugopal, J. Krishnamurthy, K.S. Rama Rao, P. Kanta Rao, J. Phys. Chem. B 106 (2002) 1024.
- [22] G. Ertl, Adv. Catal. 37 (1990) 213.
- [23] S. Narayanan, K. Krishna, Appl. Catal. A: Gen. 174 (1998) 221.
- [24] E.A. Gelder, S.D. Jackson, C.M. Lok, Catal. Lett. 84 (2002) 205.